INTERFACE MAGNON MODES IN CUBIC FERROMAGNETIC LATTICES

Malika BOUCHERRAB[1], Rebiha CHALLALI[1], Boualem BOURAHLA[1,*]

We investigate the magnonic localized phenomena at the ferromagnetic interface in crystalline cubic lattices. The interface is obtained as juxtaposition of two semi-infinites bcc and fcc lattices with atomic sites having spins in the same orientation. The crossing of the two semi-infinite cubic structures bcc and fcc can form a magnetic interface, depending on the first system to be used, either bcc-fcc, or its inverse fcc-bcc.

The breaking of translational symmetry in the direction normal to the nanojunction region gives rise to localized spin modes in the vicinity of the interface. Spin excitations in both bcc-fcc and fcc-bcc interface lattices are addressed by the matching method. The latter can be applied to the analysis of magnon diffusion, as well as to the determination of localization phenomena in the vicinity of structural inhomogeneities, surfaces and interfaces.

The localized energetic states and magnonic density of states (MDOS) are calculated for the both considered interfacial systems. The evolution of the magnetic spectra is presented as a function of the variation of the exchange integrals, along the high symmetry paths. The obtained results could provide useful information to guide research on the choice of exchange parameters, the nature and arrangement of the mesh in the fabrication of functional multilayers with multiple interfaces.

Keywords: Spin interface excitations; Ferromagnetic cubic lattices; Localized spectra; Magnonic state densities

1. Introduction

The field of computer and communications technology is predicated on the utilization of artificial nanostructures, including thin films and multilayers. Indeed, the design of nanometric objects based on magnetic materials has flourished thanks to modern ultra-high vacuum deposition techniques [1-2] and characterization techniques using the vibrating sample magnetometer (VSM) [3] or magnetic force microscope (MFM). The microelectronics or spintronic industry, which is based on silicon semiconductors, has been experiencing a frantic race towards miniaturization for the past 40 years. This can be attributed to the disparity between the physical, chemical, electronic and magnetic properties of nanometric objects and those of conventionally-sized materials. The surface

[1] Faculty of Sciences, Mouloud Mammeri University, 15000, Tizi-Ouzou, Algeria
* Corresponding author e-mail: boualem.bourahla@ummto.dz

layers and interfaces are the origin of this discrepancy, where interesting physical phenomena such as surface or interface anisotropy emerge [4] very small.
From an experimental point of view, inelastic neutron scattering measurements allow magnetic excitation spectra to be traced directly for bulk materials only [5]. Henceforth, surface or interface magnons in thin films escaped any experimental investigation. This was later made possible by the SPEELS technique (Spin-Polarized Electron Energy Loss Spectroscopy) [6]. But, the experimental breakthrough for measuring the dispersion amplitudes of surface magnons came in 2007, with the arrival of the HREELS spectrometers (High-Resolution Electron Energy Loss Spectroscopy) [7], concluding that specific magnetic responses appear at the surface or interface, called localized surface or interface states, different from the magnetic responses recorded in the bulk state of the material. The phenomena of magnetic excitations and magnonic scattering can be controlled and directed as desired, simply by controlling the way nanostructures are assembled [8-9].

To address, theoretically, the problem of spin dynamics in magnetic structures, in the presence of inhomogeneous sites or perturbed regions, one of the three methods available in the literature should be used. These methods allow for the assessment of the impact of defects and the effects of symmetry breaking. They are the slab method, Green's function method, and the matching method.
We emphasize that our research team specializes in the application of the last cited technique. We have applied it to several types of structures those exhibiting symmetry breaks, those containing implanted nanostructures and/or isolated defects, and this in the phononic, magnonic, and electronic domains.
With regard to magnetic structures, the advantage of this technique lies in its ability to accurately describe, using the same formalism, the propagation of waves through different heterogeneities and to track the phenomenon of excitation localization without any limitations on size and/or thickness.
However, Slab's method requires a large number of spin layers to guarantee the existence of a volume. In addition, Green's functions method involves a very complex mathematical formalism, which can sometimes be difficult to understand. The application of the matching method has made it possible to study numerous problems related to precession and spin excitation in magnetic structures. Based on this method, we examined the diffusion of magnons through nanocontacts in thin films and confined structures [10-12]. The localized energy states generated by a surface in cubic structures and semiconductor oxides were also determined and analyzed [13-14]. We have shown that the plane surface leads to spin resonances in the magnetic spectra.
For interfaces, we have only studied 2D scattering [15]. However, the problem of magnon localization along high symmetry directions, at interfaces joining two

semi-infinite cubic structures, with different meshes, has not been addressed. Therefore, we propose to do so in this paper.
More specifically, we analyze the localized spin states spectra generated by a ferromagnetic cubic interface that connects two ferromagnetic semi-infinite cubic lattices, bcc-fcc or its inverse fcc-bcc, as well as the local density of states as a function of the magnetic exchange parameters governing the magnetic interactions between the moments of nearby atomic spins.

The paper is organized as follows, in the next section; we present the theoretical Heisenberg model theory. In subsection 2.1, we describe the motion of spins in the two regions far from the interface, i.e., an overview of spin dynamics is recalled in the subspaces located on both sides of the interface region. Subsection 2.2 then focuses on the theoretical aspect, which addresses the properties of the interface itself. In Section 3, numerical applications are performed and discussed. The energy spectra of the localized interface states and the magnonic densities of states of the irreducible sites are determined as a function of all parameters describing the nanojunction region. In the last Section, we conclude this work.

2. Heisenberg model theory

2.1. Spin motion far from the interface

The cubic interfaces considered in this work consist of the juxtaposition of two semi-infinite bcc and fcc subsystems, along [100] direction. We assume that the lattice parameters of the two crystals located on both sides of the interface are very close ($a_{bcc} \approx a_{fcc} = a$), and that all spin moments in the ground state (low temperature) have the same orientation (ferromagnetic order). Moreover, they only differ in the values of their exchange integrals which ensure the coupling between different spin sites. We refer to this as J_{bcc}, in the perfect bcc lattice, and as J_{fcc}, in the perfect fcc lattice. It is reported that the interface area can be treated as two coupled surfaces, each having translational symmetry broken along the normal direction. Thus, the exchange integrals between the spin sites which ensure the junction between the cubic substructures are described by J_{in}. Such that $J_{in} = J_{bccfcc} = J_{fccbcc}$. A representation of the general shape of the cubic interface under study is given in Fig. 1.

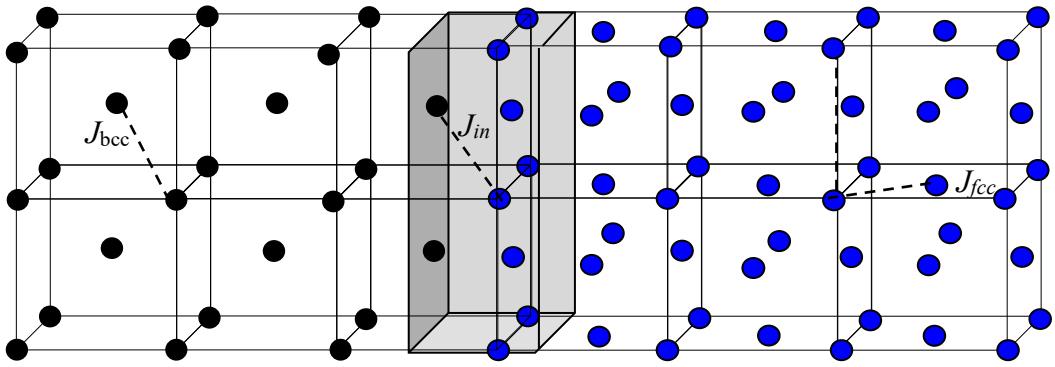

Fig. 1. Schematic representation of an interface connecting two semi-infinite cubic lattices bcc and fcc. The shaded zone denotes the nanojunction.

The most practical theoretical model that treats the spin motion with the only contribution of magnetic exchange interactions is the Heisenberg model [16], which derives from collinear magnetism, where all atomic spins are assumed to be localized, and is written as follows

$$H = -\sum_{p,p'} J_{pp'} \vec{S}_p \vec{S}_{p'} \tag{1}$$

The Heisenberg Hamiltonian is thus the summation over all exchange interactions between close neighbors, where $J_{pp'}$ is the Heisenberg exchange integral corresponding to the interaction amplitude between the spin vectors $\vec{S}_p$ and $\vec{S}_{p'}$ localized at sites p and p', respectively. Here $J_{pp'} > 0$, so the interaction promotes ferromagnetic order. It is depending on the location of the spin site in the system. The magnetic exchange is uniform, in each perfect lead, except in the interface.
By applying Eq. (1) separately to each perfect waveguide (bcc and fcc), far from the interface region, the equations for the spin dynamics may be cast in the square matrix form

$$\left[\Omega I - M(\kappa, e^{i\phi_y}, e^{i\phi_z})\right] |\vec{u}\rangle = |0\rangle \tag{2}$$

where I is the identity matrix of the same rank as the matrix dynamics M of the perfect cubic lattice, and $|\vec{u}\rangle$ denotes the vector of spin precessions. The symbols (κ, ϕ_y, ϕ_z) are, respectively, the Bloch factors, along x, y and z-directions, between neighboring sites in the unit cell. Their expressions are $(\kappa = e^{iq_x a}, e^{i\phi_y} = e^{iq_y a}, e^{i\phi_z} = e^{iq_z a})$. The constant a refers to the mesh parameter and $\vec{q}(q_x, q_y, q_z)$ defines the reciprocal space of the Brillouin zone.

The ratio $\Omega = \omega/\omega_0$ is a dimensionless frequency, where ω and ω_0 designate, respectively, the spin excitation frequency and its characteristic one.

We point out that in this work, we examine the spinwaves dispersion and magnon scattering in the structures under study along the high symmetry directions. The coordinates and paths to be followed are given in Ref.[17].
The solutions that are generated by calculating the determinant of the matrix in Eq. (2) grant access to frequencies of the precession modes as well as the dispersion curves of the spinwave in each perfect structures bcc and fcc. The results are shown in Fig. 2.

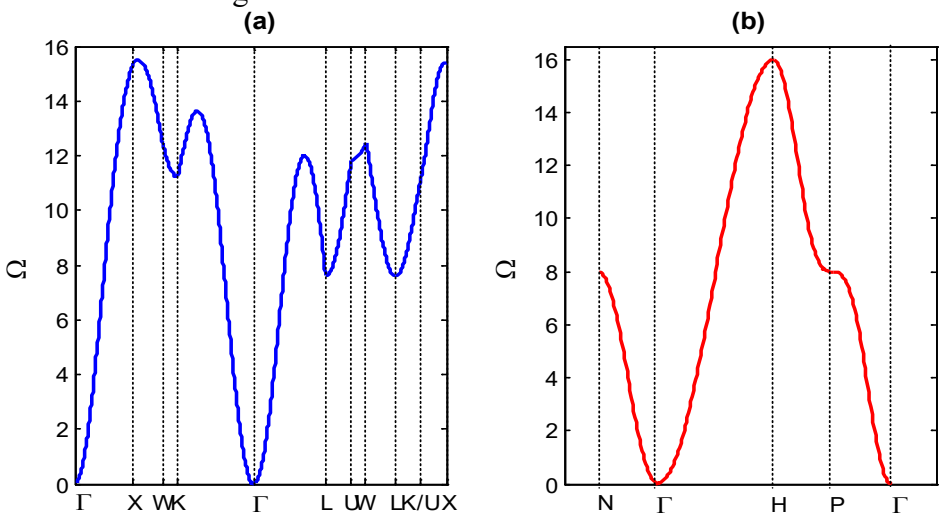

Fig. 2. Magnon dispersion curves in ferromagnetic cubic lattices, along the high symmetry directions. (a) In bcc lattice, (b) In fcc lattice.

2.1. Localized spin modes and magnonic density of states

To describe magnon scattering through a magnetic interface, we need to use all solutions of the system of spin precession equations that satisfy the condition $|\kappa| \leq 1$ (which takes into account the propagating and evanescent modes). These solutions are obtained by Gagel's method [18], which consists in linearising the initial system of equations by increasing the eigenvector basis of the two perfect lattices (located on both side of the junction zone).

To calculate the localized spin modes and the magnonic density of states at the interface spin sites, we use the analytical method, known as the matching method [10-15], based on the Green's function operator. The main element to start the procedure is based on the determination of the scattering matrix of the structure containing the interface bcc-fcc or its inverse. Often, this matrix is called Landuer scattering matrix. It is obtained by applying the formalism of the Landauer-Buttïker formalism [19]. The latter allows us to report localization spin precession phenomena and scattering spin excitation across the interface zone. The dynamics matrix can be deduced by following the steps below:

- First, we write the equations of motion of the irreducible spin sites, and those of the matching sites (sites which ensure connection between the interface domain itself and the two perfect cubic bcc and fcc structures located on either side).
- Second, we group all the equations into matrix writing.

It is noted that writing the equation of a given matching site implies the appearance of the precession amplitude of the neighboring sites positioned on the adjacent surface layers in the perfect bcc or fcc lattice. This situation leads to a rectangular matrix dynamics $M_{in}(l\times r)$, where l represents the number of spins in the interface zone and the two connection surface layers. On the other hand, r corresponds to the sum of l and the number of adjacent sites which are involved in the precession equation of motion.

We note that the matrix M_{in} elements are expressed in the spin basis vector $[|irr\rangle, |rac\rangle]$. The first part $|irr\rangle$ refers to the amplitude of the spin precessions of the irreducible sites, while the second part $|rac\rangle$ refers to the spin precessions of the two matching planes positioned on either side of the interface.

To overcome the problem of rectangular shape of the M_{in} matrix, we introduce the matching matrix (M_{ra}) which corresponds to the structure in the presence of the interface. (We recall that the matching matrix consists of expressing the precession amplitudes of all spins (numbered r) as a function only of the amplitudes of the irreducible sites and the matching quantities which characterize the two subspaces to the left and the right of the interface zone (the eigenvalues and the eigenvectors of the dynamics matrices of the perfect bcc and fcc structures). Therefore, M_{ra} will have the dimension ($r\times l$)).

To access to the dynamic properties of spins in the bcc-fcc interface structure or its inverse, we perform the matrix product $M_{in}.M_{ra}$. This allows us to obtain a square matrix M_{sq}, of dimension ($l\times l$).

$$M_{in}(l\times r).M_{ra}(r\times l)=M_{sq}(l\times l) \tag{3}$$

Calculating the determinant of the last square matrix (M_{sq}) allows obtaining the localized spin modes generated by the spin interface layers, according the next equation

$$\det\left[M_{sq}(l\times l)\right]=0 \tag{4}$$

The spectra of the localized spin modes relating to the two studied interfaces, bcc-fcc and fcc-bcc, respectively, are plotted in Figs. 3 and 4.

Furthermore, we point out that knowledge of the M_{sq} matrix is important, since it is the key to access several magnonic spectra of the interface structure, such as transmission/reflection coefficients, spin wave transmittance and the magnonic density of states (MDOS). The first two properties are not reported in this present work; we are rather interested in MDOS. The later is defined as the number of magnonic states of the material under study.

The commonly used method for determining spectral and state densities, per spin site, relies on Green's functions. This method is based on the local Green's operator in real space, for a given wavevector [20]. In this work, the mentioned densities are derived from the square matrix of equation (3). They are expressed as follows:

$$\rho_{\alpha,\beta}^{p,p'}(\Omega,e^{j\phi_y},e^{j\phi_z})=\frac{-1}{\pi}\sum_{\alpha}P_{\alpha_r}^{p}P_{\beta_r}^{p'}\delta(\Omega-\Omega_r)=\frac{-1}{\pi}\lim_{\varepsilon\to 0^+}\left\{\mathrm{Im}\left[G_{\alpha\beta}^{pp'}(\Omega+j\varepsilon,e^{j\phi_y},e^{j\phi_z})\right]\right\} \quad (5)$$

The quantities $P_{\alpha r}^{p}$ and $P_{\beta r}^{p'}$ denotes the α, β-components of the polarisation vectors for p, p' spin sites at the magnon branch Ω_r. The notation $G_{\alpha\beta}^{pp'}$ refers to the Green's operator defined from the matrix M_{sq} as follow

$$G(\Omega+j\varepsilon,\phi_y,\phi_z)=\left[(\Omega+j\varepsilon)I-M_{sq}\right]^{-1} \quad (6)$$

Analytically, the spectral density per spin site is calculated over the trace of the matrix M_{sq} for $p \equiv p'$, where p runs over the sites of the irreducible set of spins in the interfacial domain.

The magnonic density of spin states for spin site p, denoted as $D(\Omega)$, is calculated as sum over the trace of the spectral density matrix

$$D(\Omega)=S_{\alpha,\alpha}^{p,p'}(\Omega,e^{j\phi_y},e^{j\phi_z})=\frac{-1}{\pi}\sum_{\phi_y}\sum_{\phi_z}\sum_{\alpha}\lim_{\varepsilon\to 0^+}\left\{\mathrm{Im}\left[G_{\alpha\alpha}^{pp}(\Omega+j\varepsilon,e^{j\phi_y},e^{j\phi_z})\right]\right\} \quad (7)$$

In all cases, it should be noted that the information obtained depends on the incidence of the spinwaves propagation in the considered interface lattices.

The MDOS are calculated and presented, in Figs. 5-6, for the two irreducible sites of the interface zone.

3. Numerical results and discussions

In the perfect bcc and fcc structures, we note that each branch propagates in its specific interval (Fig. 2). The dispersion mode of the bulk magnons is acoustic in the two ferromagnetic cubic structures, it tends towards zero, when the wave vector tends towards the center of the Brillouin zone ($\Omega \to 0$, for $q_x \to \Gamma$).

When we change the propagation path, the propagation mode of spin waves becomes optical; the normalized energy is different from zero ($\Omega \neq 0$). This is observed along the *HP* for the bcc lattice and along the XK, LW and LX paths for the fcc lattice. Consequently, the energy carried by the spin wave differs from one crystallographic structure to another. This is expected because the exchange energy governing a ferromagnetic cubic system is a direct function of the coordination number between neighboring spins and the exchange couplings.

At the level of surfaces and interfaces, due to the reduced number of neighbors, modifications appear such as a narrowing of the conduction band and an increase in the density of magnonic states. These modifications lead to large variations in the magnetic properties of ferromagnetic structures and assemblies.

Our objective in this work is to simulate and analyze the phenomenon of spin and magnon localization across a ferromagnetic interface, in two types of interfaces bcc-fcc and its inverse fcc-bcc, for the three possibilities of magnetic exchange constants between different neighboring spin sites. As indicated in the theoretical aspect, Eq. (4) gives access to the energies of the localized interface branches as a function of the magnetic couplings between spins of the interface region and spin sites of the two perfect subspaces located on both sides of the nanojunction zone.
The results are plotted in Figs. 3-4 for the cubic system interfaces bcc-fcc and fcc-bcc, respectively. Note that the incident spins wave follows the [100] direction. It is important to consider the direction of diffusion of the incident wave when the mesh is crossed because, as we will see, the direction of propagation of the spin wave and the crystal structure of the nanojunction will play a major role in the scattering and magnon localization phenomena.

In order to work with normalized energies, it is useful to define the following ratios for the perturbed waveguides $\gamma_{in} = \frac{J_{in}}{J_{bcc}}$ on the bcc side and $\gamma_{in} = \frac{J_{in}}{J_{fcc}}$ on the fcc side. The possibilities analyzed are for the following ratio values of the interaction forces.

(a) $\gamma_{in} < 1$, in order to describe the softening interactions at the interface,
(b) $\gamma_{in} \approx 1$, to report the homogeneity case at the interface.
(c) $\gamma_{in} > 1$, to examine the hardening situation at the interface.

For the numerical simulations performed, we chose variations of approximately 20% between the physical parameters characterizing the interface layers, compared to the two perfect layers located on either side of the interfacial region. More precisely, the numerical analysis is conducted for a comparable spin intensity $S_{fcc} = S_{bcc}$ (since the planes of the interface region are either fcc or bcc), and we explored the three possible values of magnetic coupling, thus determining a spin environment for the interface sites (20% higher, similar, or 20% lower). This constitutes a plausible situation for most surfaces when anisotropy is taken into account.
To carry out our numerical calculations and simulate the behavior of spin waves at the interface of the bcc-fcc system, in the cited three possibilities (a)-(c), we introduced the following parameters into our calculation programs:
(a) $J_{bcc} = 1.0$, $S_{bcc} = S_{fcc}$, $J_{fcc} = 0.8 \times J_{bcc}$, $J_{int} = (J_{bcc}+J_{fcc})/2 = 0.9$
(b) $J_{bcc} = 1.0$, $S_{bcc} = S_{fcc}$, $J_{fcc} \approx J_{bcc}$, $J_{int} = (J_{bcc}+J_{fcc})/2 = 1.0$
(c) $J_{bcc} = 1.0$, $S_{bcc} = S_{fcc}$, $J_{fcc} = 1.2\ J_{bcc}$, $J_{int} = (J_{bcc}+J_{fcc})/2 = 1.1$.
We mention that our numerical calculations are not based on any particular experiment. However, it is interesting to note that the most relevant experimental systems currently available for the theoretical study of localized spin states would

probably be interfaces resulting from the junction of surfaces with magnetic symmetry breaking and point magnetic contacts.

Although the possible values of spin intensity and interaction environment (softening, homogeneous, and hardening) are not exact values, which can be significant in some magnetic materials; each choice represents a reasonable working value to illustrate our calculations by simulating spin dynamics in certain interface configuration models.

It should be noted that the developed programs for our calculations can be run for all possible values of magnetic exchange and spin intensity.

Dividing by the exchange constant of the system from which the excitatory spinwave is incident, we obtain the normalized quantities (described by the values 0.8, 1.0 and 1.2). Further, in the layers composing the interface, the coupling constant between the spins is taken as an arithmetic mean (which gives a variation of the order of 10% compared to the perfect waveguides fcc and bcc).

In the system bcc-fcc, the normalization of the exchange integrals is ensured by J_{bcc}. The later corresponds to the coupling in the semi-infinite bcc system, located before the interface zone, and ensures the diffusion of the spin wave towards the second semi-infinite fcc lattice. The obtained results are plotted in Fig. 3.

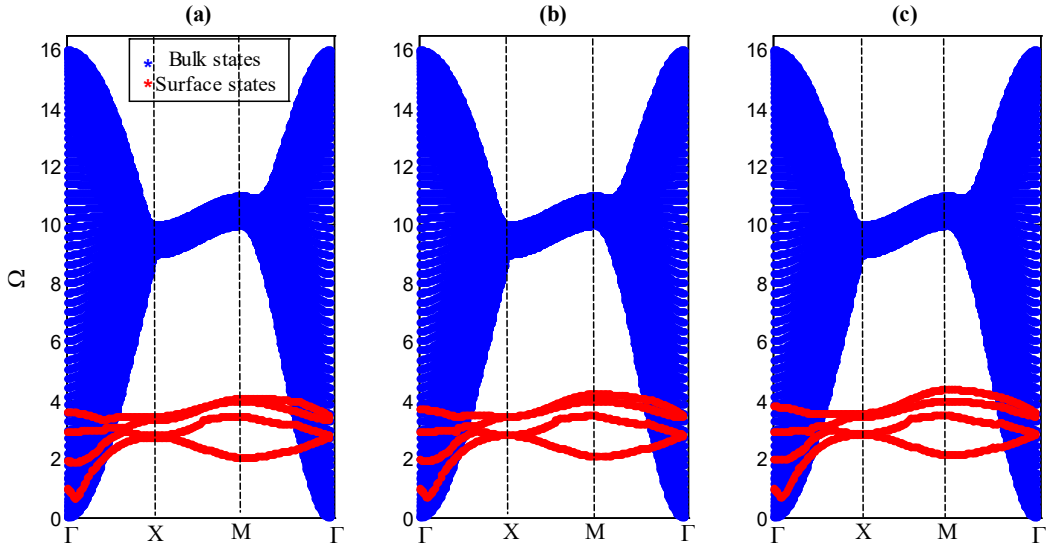

Fig. 3. Normalized spinwave energies generated by the interface zone in bcc-fcc ferromagnetic lattice are presented along [100] juxtaposition direction. The localized spin dispersion branches are simulated based on the exchange integrals in the scattering zone. Further, the bulk-related band of the perfect scattering waveguide (bcc) is shown.

(a) We simulated a softening situation that corresponds to the ratio $\gamma_{in} < 1$.

(b) We reported the homogenous case $\gamma_{in} \approx 1$.

(c) We examined a hardening situation that given by the ratio $\gamma_{in} > 1$.

In other hand, the impact of the surface, in the structure fcc-bcc, is realized in a similar way to the previous case. Except that in this case, we normalized the exchange integrals by J_{fcc}, since it is the semi-infinite fcc lattice that is located before the interface and ensures the propagation of the spin wave towards the semi-infinite bcc lattice. Explicitly, we used the following parameters:

(a) $J_{fcc} = 1.0$, $S_{fcc} = S_{bcc}$, $J_{bcc} = 0.8 \times J_{fcc}$, $J_{int} = (J_{bcc}+J_{fcc})/2 = 0.9$,

(b) $J_{fcc} = 1.0$, $S_{fcc} = S_{bcc}$, $J_{bcc} \approx J_{fcc}$, $J_{int} = (J_{bcc}+J_{fcc})/2 = 1.0$,

(c) $J_{fcc} = 1.0$, $S_{fcc} = S_{bcc}$, $J_{bcc} = 1.2 \times J_{fcc}$, $J_{int} = (J_{bcc}+J_{fcc})/2 = 1.1$.

The results of the localized states corresponding to the fcc-bcc structure are plotted in Fig. 4.

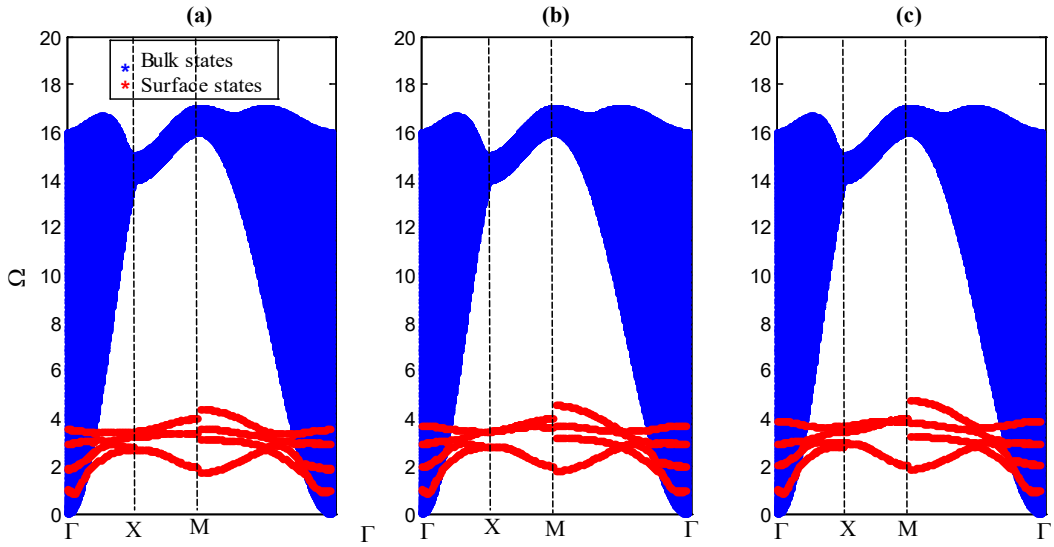

Fig. 4. Normalized spinwave energies generated by the interface zone in fcc-bcc ferromagnetic lattice are presented along [100] juxtaposition direction. The localized spin dispersion branches are simulated based on the exchange integrals in the scattering zone (from softening to hardening). Further, the bulk-related band of the perfect scattering waveguide (fcc) is shown.
(a) We simulated a softening situation that corresponds to the ratio $\gamma_{in} < 1$.
(b) We reported the homogenous case $\gamma_{in} \approx 1$.
(c) We examined a hardening situation that given by the ratio $\gamma_{in} > 1$.

The three possibilities make a sweep of all the situations that can be encountered. Cases (a) and (c) correspond, respectively, to the softening and hardening of the magnetic exchange interactions in the interface domain itself. Our objective is to describe the response of the magnonic properties of the interface and the behavior of the irreducible spin sites located in the planes that form the interface when the exchange integrals vary. While, in case (b), the exchange interactions are taken to be comparable (very close values) throughout the system. This allows us to highlight the impact of the homogeneity of the

magnetic exchange. It is reported that analytically, the broken periodicity induced by the presence of surfaces that create the interface in a spin system leads to the appearance of additional mathematical solutions. These solutions have a complex wave vector $\vec{q}(q_x, q_y, q_z)$ in the direction normal to the interface. As a result, the wave functions will be evanescent and the electrons will be localized in the foreground of the system relevant to the nanojunction, giving rise to so-called interface localized states.

In the case of the bcc-fcc interface and its inverse fcc-bcc, the bulk magnon spectrum, for each structure, is a band that is represented together with the magnon branches generated by the surface layers. Our approach allows to detect the effect and impact of the surface on spin waves, and also to study the behavior of spin excitations and variations of spin precession amplitudes and their responses to local changes in surface magnon properties, when the number of nearest neighbors decreases. In Figs. 3-4, the spectra relating to the interface layers are given as red branches, on the other hand, the bulk states are propagation bands (continuum) in blue color. In both cases of examined interfaces, we find that the localized states are less energetic than the bands allowed for the bulk of the perfect bcc and fcc lattices. This is explained by the annihilation of the precession amplitudes when passing from one mesh to another. We also conclude that in both types of interfaces, multiple oscillations are less favored; on the other hand, extended transmissions are more marked. Moreover, the low frequencies of the branches of the localized states can be justified by the large wavelength of the spin wave compared to the distance between first nearest neighbors which is of the order of $\frac{a}{\sqrt{2}}$ for the fcc and $\frac{a}{\sqrt{3}}$ for the bcc.

Comparing Fig. 3 with Fig. 4, we observe that the shape of the bulk band is very different for bcc and fcc structures. For each cubic lattice, the limits of the magnonic frequency intervals coincide with the limits of the obtained dispersion curves. Localized spin states are very sensitive to the mesh of the first subspace in which the spin wave propagates toward the interface domain. This gives rise to particular characteristics specific to each interface system bcc-fcc or its inverse. Furthermore, we observe that in all considered cases, the localized spin branches exhibit oscillations that depend on the exchange parameters in the interface region. Some branches of localized states interfere with the bulk states. These are called resonant states. However, interface branches are the states that appear after symmetry breaking. We recall that our two interfaces are the result of the juxtaposition of semi-infinites bcc and fcc subsystems. Branch analysis leads to the identification of three categories of interface spectra modes directly related to the two contacting surfaces:

- Branches whose frequencies are within the limits of the bulk band.
- Branches whose frequencies are lower than the magnon modes of the perfect bcc and fcc systems.
- Branches whose modes interfere with the spinwave propagation modes.

The changes in the position and shape of the spin branches are the signature of a confinement effect due to the variation of the coordination in each semi-infinite cubic structure, along the axis normal to the surface layers in the interface domain.

In the three possibilities studied for the simulated exchange integrals, the interface magnonic spectra become more energetic and the localized states shift towards higher frequencies, with increasing exchange in the layers adjacent to the irreducible sites. By analogy with the studies of localized phenomena, we find three main types of surface and interface magnonic states in the two studied interfaces: bcc-fcc and fcc-bcc with ferromagnetic coupling: (i) Rayleigh-type spin mode [21], (ii) Fuchs-Kliewer-type spin branches [22], and (iii) Microscopic interface spin branches [23].

Modes (i) and (ii) are characterized by long penetration in both perfect bcc and fcc lattices. Moreover, Rayleigh modes are often located below the acoustic branches, as in the case of softening, as shown in Figs. 3a and 4a.

By definition, Fuchs-Kliewer modes are located on the optical branches. Modes (iii) are located in the continuous space of the magnonic spectrum of bcc and fcc crystals.

In the second part of this work, we determined and presented the magnonic densities of states (MDOS). The results are given in Figs. 5 and 6. The calculation was done for the two spin sites that constitute the irreducible sites (in the interfacial region). The MDOS of the system bcc-fcc are presented in Fig. 5. Whereas, the MDOS of its inverse fcc-bcc are plotted in Fig. 6. The spectra are arranged in columns to describe the variation of the magnetic exchange γ_{in} (from softening in the left to hardening in the right column and homogenous in the center). The rows correspond to the two spin layers located in the interface domain.

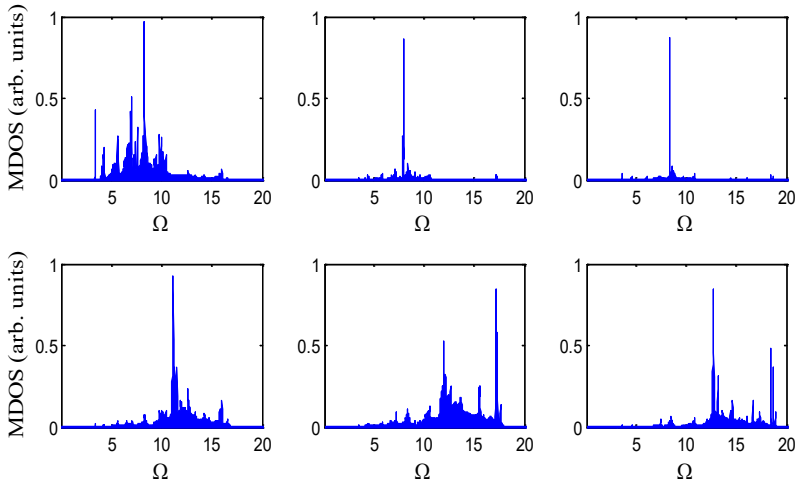

Fig. 5. Response of the magnonic density of states (MDOS) of the irreducible spin sites located in the interface region to the variation of the spin interaction parameters, in the interface domain of the bcc-fcc ferromagnetic lattice. The three columns describe the variation of the magnetic exchange and the rows indicate the spin sites belonging the two planes of the interface region. Site (1) is located in the bcc lattice, while site (2) is in the fcc lattice.

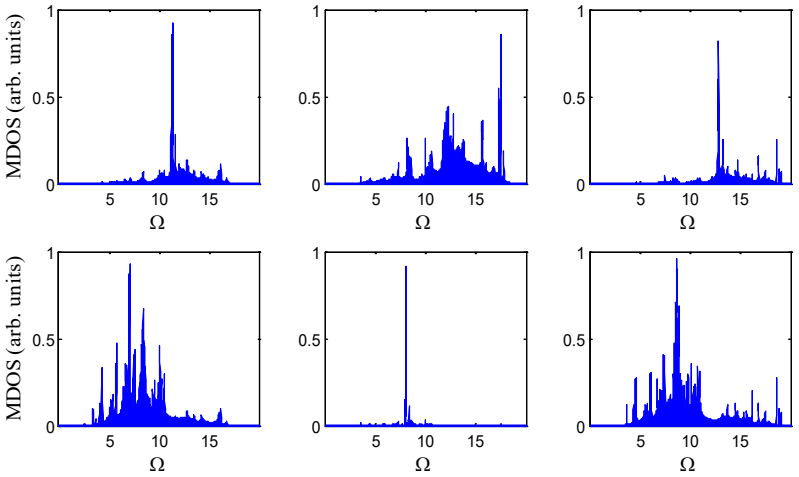

Fig. 6. Same as Fig. 5, but for the fcc-bcc ferromagnetic lattice. Here the spin site (1) is located in the fcc lattice, while site (2) is in the bcc lattice.

In the two Figs. 5-6, the MDOS results, for the two irreducible sites, present specific characteristics and others common to the two interface systems. In Fig. 5, which corresponds to the bcc-fcc crossing, we see that at low frequencies, the site (1) is excited first, compared to the second irreducible spin site (2), which is positioned on the 2nd layer, located in the second fcc mesh subspace. As the frequency increases, we notice that the precession amplitude of site (2) increases in intensity. Moreover, with the hardening of the magnetic

exchange integrals in the interface domain itself, the intensity and amplitudes of the sites decrease for site (1) and an opposite behavior is observed for site (2). This is largely attributed to the own frequency of the fcc system (where the spin wave velocity propagation is different compared to the bcc mesh subspace) and the other part comes from the magnonic transmittance via the interface.
In other hand, in Fig. 6, at very low frequencies, we observe that the MDOS spectra of the two spin sites are almost zero. Then, the spectra exhibit non-uniform fluctuations with unpredictable behavior as the coupling constants vary.
The position $\Omega = 12$ constitutes a collective oscillation frequency of the two sites (1) and (2), and this in both cases of interface crossing. By comparing the obtained results, the resonance peaks of the irreducible sites with the largest amplitude are observed at identical frequency positions.
Finally, the MDOS peaks strongly depend on the magnetic exchange and the mesh of the structure which ensures the propagation of the incident spinwave towards the interface zone. The interferences between the surface spin layers and the bulk states are at the origin of the organization of the transmission/reflection of the magnonic transport via interfaces.

6. Conclusions

The spin dynamics of a model interface connecting two different bcc and fcc cubic crystallizations is presented. We rigorously establish the evanescent precessional spin modes at the interface region, which ensures the nanojunction, by the matching technique. The advantage of the used method, compared to others, in addition to being transparent at all stages of the calculations, is expressed by an exact and rigorous analytical formulation of the amplitudes of precessions of the spin vectors in the structure under study.
From the matrix dynamics, we derived the localized spin states and the magnonic density of states (MDOS) of the spins representing the sites located in the irreducible zone. The magnetic spectra are determined and discussed based on the various parameters characterizing the interface itself. Certain spectral oscillations are identified as Rayleigh modes parallel to the interface region.

Depending on the crystallographic structure of the mesh of the semi-infinite cubic structure (fcc or bcc), the results obtained show that the subspace in which the incident wave propagates toward the interface imposes its scattering frequencies on the structure with the interface. Furthermore, certain peaks observed in the magnonic spectra (localized spin states and MDOS) characterize particular oscillations. Some of them result from the interactions between the localized spin states generated by the interface domain, with the propagating modes of the continuum. At the end, we can say that the calculated magnonic spectra could guide experimenters by providing useful information concerning the

exchange parameters at the interface, propagation direction and the impact of the mesh.

Acknowledgments

The authors would like to thank Linea Boussair for her support.

REFERENCES

[1] *J. Moritz, B. Dieny, J. P. Nozieres, S. Landis, A. Lebib, Y. Chen*, Domain structure in magnetic dots prepared by nanoimprint and e-beam lithography, J. Appl. Phys. Vol. **91**, Iss. 10, 2002, 7314-7316

[2] *R. W. Schwartz, T. Schneller, R. Waser*, Chemical solution deposition of electronic oxide films, Comptes Rendus Chimie Vol. **7**, Iss. 5, 2004, 433-461

[3] *W. S. Goree, M. Fuller*, Magnetometers using RF-driven squids and their applications in rock magnetism and paleomagnetism, Rev. Geophys. Vol. **14**, Iss. 4, 1976, 591-608

[4] *H. Terada, S. Ohya, L. D. Anh, Y. Iwasa, M. Tanaka*, Magnetic anisotropy control by applying an electric field to the side surface of ferromagnetic films, Sci. Rep. Vol. **7**, Iss. 1, 2017, 5618

[5] *A. Khitun, K. L. Wang*, Non-volatile magnonic logic circuits engineering, J. Appl. Phys. Vol. **110**, Iss. 3, 2011, 034306

[6] *G. L. Squires*, Introduction to the theory of thermal neutron scattering, Courier Corporation, 1996

[7] *M. Plihal, D. L. Mills, J. Kirschner*, Spin wave signature in the spin polarized electron energy loss spectrum of ultrathin Fe films: theory and experiment, Phys. Rev. Lett. Vol. **82**, Iss. 12, 1999, 2579

[8] *E. Albisetti, D. Petti, G. Sala, R. Silvani, S. Tacchi, S. Finizio, R. Bertacco*, Nanoscale spin-wave circuits based on engineered reconfigurable spin-textures, Comm. Phys. Vol. **1**, Iss. 1, 2018, 56

[9] *A. Hirohata, K. Yamada, Y. Nakatani, I. L. Prejbeanu, B. Diény, P. Pirro, B. Hillebrands*, Review on spintronics: Principles and device applications, J. Mag. Mag. Mat. Vol. **509**, 2020, 16671110

[10] *B. Bourahla, A. Khater, R. Tigrine, O. Rafil, M. Abou Ghantous*, Magnons coherent scattering via atomic nanocontacts, J. Phys. Cond. Matter Vol. **19**, Iss. 26, 2007, 266208 – 266220

[11] *O. Nafa, B. Bourahla, A. Khater*, Scattering properties induced by an asymmetric nanowell on ferromagnetic ultrathin film, J. Phys. Chem. Solids Vol. **74**, Iss. 3, 2013, 395–401

[12] *L. Ferrah, B. Bourahla, S. Blizak*, Modeling and Simulation of Magnons Scattering Across Shear Spins in Multilayered Ferromagnetic Slabs, Spin Vol. **11**, Iss. 4, 2021, 2150028

[13] *F. Chelli, B. Bourahla, A. Khater*, Computational of localized spinwaves at a stepped surface of an antiferromagnetic metallic monoxide, Inter. J. Modern Phys. B Vol. **34**, Iss. 9, 2020, 2050080

[14] *R. Challali, S. Sait, B. Bourahla, L. Ferrah*, Localized Surface Magnon Modes in Cubic Ferromagnetic Lattices, Spin Vol. **12**, Iss. 1, 2023, 2350001

[15] *L. Djebala, B. Bourahla*, Magnons transmission across soliton domain in 2D triangular ferromagnetic waveguides, Spin Vol. **11**, Iss. 2, 2021, 2150014

[16] *J. H. Van Vleck*, Quantum mechanics: The key to understanding magnetism, Science Vol. **201**, Iss. 4351, 1978, 113-120

[17] *W. Setyawan, S. Curtarolo*, High-throughput electronic band structure calculations: Challenges and tools, Comput. Mat. Sci. Vol. **42**, Iss. 2, 2010, 299-312
[18] *F. Gagel, K. Maschke*, Finite-difference approach to edge-state transport in quantum wires and multiterminal devices, Phys. Rev. B Vol. **52**, Iss. 3, 1995, 2013
[19] *R. Landauer*, Conductance determined by transmission: probes and quantised constriction resistance, J. Phys.: Condensed Matter Vol. **1**, Iss. 43, 1989, 8099
[20] *S. Sait, Bourahla*, Spin waves propagation through honeycomb-shaped nanocontacts in 2D-Heisenberg ferromagnets, Spin Vol. **15**, Iss. 3, 2025, 255007
[21] *Y. Au, O. S. Latcham, A. V. Shytov, V. V. Kruglyak*, Resonant scattering of surface acoustic waves by arrays of magnetic stripes, J. Appl. Phys. Vol. **134**, Iss. 23, 2023, 233904
[22] *F. Mazzola, C. M. Yim, V. Sunko, S. Khim, P. Kushwaha, O. J. Clark, L. Bawden, I. Marković, D. Chakraborti, T. K. Kim, M. Hoesch, A. P. Mackenzie, P. Wahl, P. D. C. King*, Tuneable electron–magnon coupling of ferromagnetic surface states in $PdCoO_2$, npj Quantum Mat. Vol. **7**, Iss. 1, 2022, 20
[23] *A.V. Chumak*, In Spintronics Handbook, 2nd Edition: Spin transport and magnetism, CRC Press, 2019, pp. 247-302